

Brief Communication

Insights into autotaxin- and lysophosphatidate-mediated signaling in the pancreatic ductal adenocarcinoma tumor microenvironment: a survey of pathway gene expression

Matthew GK Benesch^{1*}, Rongrong Wu^{1,2*}, Colin J Rog¹, David N Brindley³, Takashi Ishikawa², Kazuaki Takabe^{1,2,4,5,6,7}

¹Department of Surgical Oncology, Roswell Park Comprehensive Cancer Center, Buffalo, New York 14263, USA; ²Department of Breast Surgery and Oncology, Tokyo Medical University, Tokyo 160-8402, Japan; ³Cancer Research Institute of Northern Alberta, Department of Biochemistry, University of Alberta, Edmonton, Alberta T6G 2S7, Canada; ⁴Department of Gastroenterological Surgery, Yokohama City University Graduate School of Medicine, Yokohama 236-0004, Japan; ⁵Division of Digestive and General Surgery, Niigata University Graduate School of Medical and Dental Sciences, Niigata 951-8520, Japan; ⁶Department of Breast Surgery, Fukushima Medical University School of Medicine, Fukushima 960-1295, Japan; ⁷Department of Surgery, University at Buffalo Jacobs School of Medicine and Biomedical Sciences, State University of New York, Buffalo, New York 14263, USA. *Equal contributors.

Received June 22, 2024; Accepted August 7, 2024; Epub August 25, 2024; Published August 30, 2024

Abstract: Lysophosphatidate (LPA)-mediated signaling is a vital component of physiological wound healing, but the pathway is subverted to mediate chronic inflammatory signaling in many pathologies, including cancers. LPA, as an extracellular signaling molecule, is produced by the enzyme autotaxin (ATX, gene name *ENPP2*) and signals through six LPA receptors (LPARs). Its signaling is terminated by turnover via the ecto-activity of three lipid phosphate phosphatases (LPPs, gene names *PLPP1-3*). Many pharmacological developments against the LPA-signaling axis are underway, primarily against ATX. An ATX inhibitor against pancreatic ductal adenocarcinoma (PDAC), a very aggressive disease with limited systemic therapeutic options, is currently in clinical trials, and represents the first in-class drug against LPA signaling in cancers. In the present study, we surveyed the expression of ATX, LPARs, and LPPs in human PDACs and their clinical outcomes in two large independent cohorts, the Cancer Genome Atlas (TCGA) and GSE21501. Correlation among gene expressions, biological function and the cell composition of the tumor microenvironment were analysed using gene set enrichment analysis and cell cyber-sorting with xCell. *ENPP2*, *LPAR1*, *LPAR4*, *LPAR5*, *LPAR6*, *PLPP1*, and *PLPP2* were significantly elevated in PDACs compared to normal pancreatic tissue, whereas *LPAR2*, *LPAR3*, and *PLPP3* were downregulated (all $P \leq 0.003$). Only *ENPP2* demonstrated survival differences, with overall survival favoring *ENPP2*-high patients (hazard ratio 0.5-0.9). *ENPP2* was also the only gene with enriched gene patterns for inflammatory and tissue repair gene sets. Epithelial (cancer) cells had increased *LPAR2*, *LPAR5* and *PLPP2* expression, and decreased *ENPP2*, *LPAR1*, *PLPP1*, and *PLPP3* gene expression (all $P < 0.02$). Tumor fibroblasts had increased *ENPP2*, *LPAR2*, *LPAR4*, *PLPP1*, and *PLPP3* expression and decreased *LPAR2*, *LPAR5*, and *PLPP2* expression in both cohorts (all $P \leq 0.01$). Immune cell populations were not well correlated to gene expression in PDACs, but across both cohorts, cytolytic scores were increased in high-expressing *ENPP2*, *LPAR1*, *LPAR6*, *PLPP1*, and *PLPP3* tumors ($P < 0.01$). Overall, in PDACs, *ENPP2* may switch from an anti-to-pro tumor promoting gene with disease progression. *LPAR2* and *PLPP2* inhibition are also predicted to have potential therapeutic utility. Future multi-omics investigations are necessarily to validate which LPA signaling components are high-value candidates for pharmacological manipulation in PDAC treatment.

Keywords: Bioinformatics, drug candidates, lysophosphatidic acid, prognostic biomarkers, pancreatic cancer, stroma

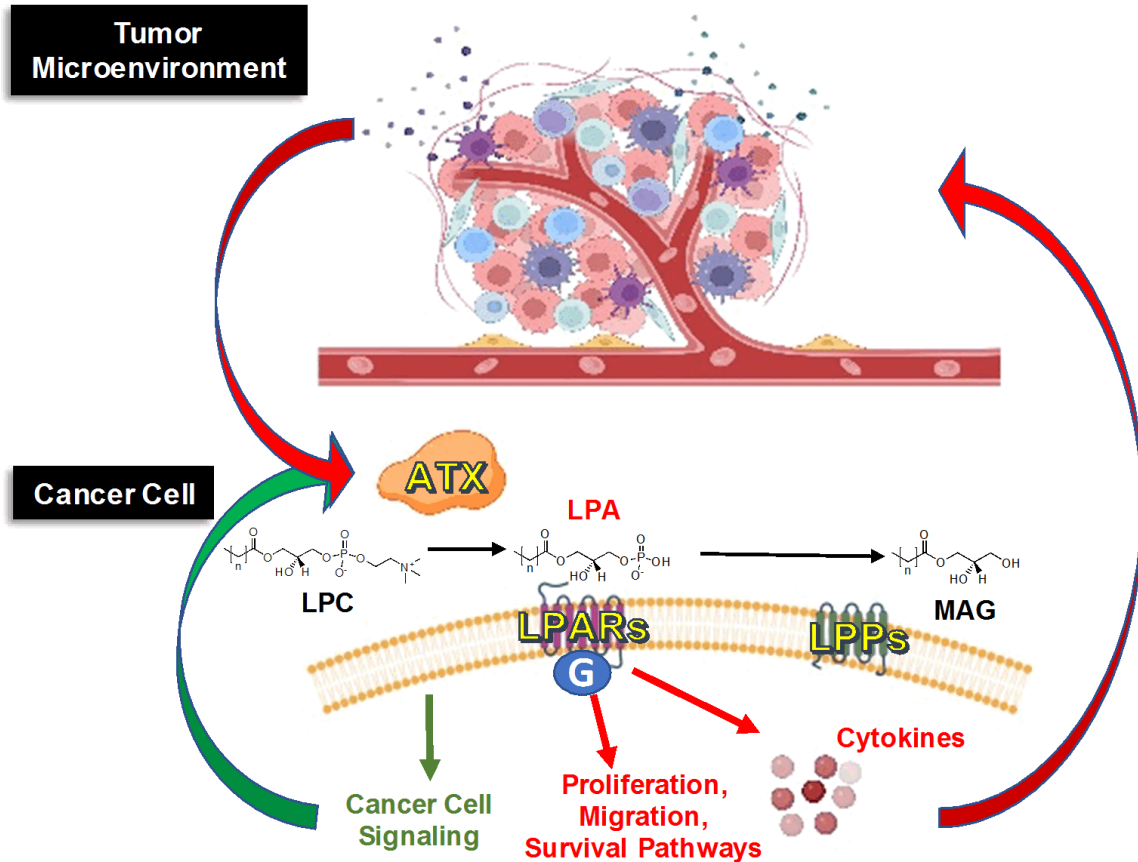


Figure 1. Overview of lysophosphatidate (LPA) signalling in the cancer and the surrounding tumor microenvironment. Extracellular LPA is produced by the lysophosphatidase D activity of the extracellular enzyme autotaxin (ATX) from plasma lysophosphatidylcholine (LPC). LPA signals through six G-protein receptors (LPARs) to activate many signaling pathways involved in cancer pathogenesis. LPA signaling is terminated by its breakdown into monoacylglycerol (MAG) via the ecto-activity of the lipid phosphate phosphatases (LPPs). ATX can be produced by cancer cells in an autocrine fashion by upregulated carcinogenic pathways, including LPA induced cytokine-mediated signaling, establishing a positive feedback loop. Cytokines within the surrounding tumor microenvironment can also induce ATX upregulation in tumor stroma for paracrine-mediated LPA signaling in cancer cells.

Introduction

Pancreatic ductal adenocarcinoma (PDAC) is an aggressive cancer that has not benefited well from continued advances in multimodal therapeutic options, with 5-year overall survival rates essentially plateaued at about 11% [1]. Although it is the tenth most diagnosed cancer, it is third in annual cancer deaths, and is projected to overtake colorectal cancer for second place before the end of the decade [1, 2]. Extensive research efforts are ongoing to overcome this aggressive tumor biology defined by its dense desmoplastic tissue and low tumor mutational burden, which both support a pro-survival milieu and tumor microenvironment [3-5].

Lysophosphatidate (LPA) functions as an extracellular bioactive lipid with numerous physiological roles central to proper embryogenesis and wound healing [6, 7]. However, these mechanisms are readily hijacked in malignancies to fuel pathways of chronic inflammation to both promote cancer progression and metastasis, and loss of efficacy for both chemotherapy and radiotherapy regimens [8]. Extracellular LPA is produced primarily from albumin-bound lysophosphatidylcholine (LPC) by the lysophospholipase D activity of autotaxin (ATX, gene name *ENPP2*) [9, 10] (Figure 1). ATX, primarily produced within the local cellular microenvironment, interacts with extracellular-membrane integrins to concentrate LPA production within the vicinity of the targeted cells [11]. LPA then

signals through six known G-protein coupled receptors (LPARs, gene names *LPAR1-6*) to elicit its mechanistic effects [12] (**Figure 1**). Receptor affinity to differing G-protein combinations result in synergetic, redundant, and antagonistic intracellular responses that ultimately define the nature of the LPA-signaling transduction cascade [6, 13]. Extracellular LPA-mediated signaling is terminated by its degradation into monoacylglycerols (MAGs) and inorganic phosphates by the ecto-activities of three unique lipid phosphate phosphatases (LPPs, gene names *PLPP1-3*), particularly LPP1 [14] (**Figure 1**).

In general, the LPA signalling cascade is upregulated in aggressive cancers, resulting in a tumor microenvironment that favors disease progression [8, 10, 15]. This occurs via several concurrent mechanisms. First, LPA concentrations are typically increased through increased ATX production [16]. This ATX can either be overexpressed by the cancer cells themselves, as seen in melanoma, thyroid carcinoma, hepatocellular carcinoma, and glioblastoma multiforme. Alternatively, tumor-induced inflammation increases ATX synthesis by cells in the surrounding tumor stroma such as in breast cancer and PDAC [6, 7, 15]. Additionally, ATX is within the top 40-50 most upregulated genes in both locally invasive and metastatic tumors [17, 18]. This additional LPA signals to elicit the mechanisms of cancer progression and therapy resistance through an enriched cancer cell LPAR profile [19]. LPP1 and LPP3 tend to be overall suppressed in most cancers, resulting in decreased ecto-LPP activity and therefore less turnover of LPA [14, 20, 21]. LPP2 functions differently and it is increased in tumors resulting in increased rates of S-phase entry through the cell cycle via upregulation of transcription by c-Myc [20, 22, 23].

The LPA pathway has been the target of much therapeutic development over the past 20 years for both cancer and chronic inflammatory diseases [6, 9]. Inhibitors against ATX and the LPARs have been studied in clinical trials, primary for idiopathic pulmonary fibrosis (IPF) [24]. Zirtaxestat, also known as GLPG1690, was the first ATX inhibitor to enter clinical trials, culminating into two phase III double-blinded and placebo-controlled trials combining zirtaxestat with standard of care therapies for IPF

(ISABELA 1 and 2) [25]. Additionally, there are at least two other ATX inhibitors (cudetaxestat or BLD-0409 and BBT-877) currently in phase II trials for IPF, with results expected in mid-to-late 2024 [26, 27]. Another ATX inhibitor, IOA-289, has been shown to inhibit tumor growth and lung and bone metastases in synergistic immunocompetent orthotopic murine models of breast cancer [28, 29], similar to other ATX inhibitors trialed in pre-clinical settings [30, 31]. IOA-289 has also been shown to reduce gastrointestinal cancer progression in pre-clinical models, including those for PDAC [32]. IOA-289 has since entered a phase 1b, open label, dose-escalation study in combination with gemcitabine/nab-paclitaxel, a standard of care treatment regimen [33], in patients with metastatic PDAC [34]. This clinical trial represents the first LPA pathway inhibitor used in cancer therapy.

Compared to most other common cancer types, the role of LPA signaling in the PDAC tumor microenvironment has not been as well studied. We have previously explored the role of mRNA expression in PDAC using *in silico* research methodologies [35-38]. We have also used these techniques to explore ATX, LPAR, and LPP expression in human breast tumors, thereby allowing for meaningful comparisons to the evolving body of literature in pre-clinical models [39-41]. In this study, we combine our expertise from these investigations to survey the effects of LPA signaling in PDACs by tumor cell populations using large databases of two independent cohorts. We develop novel insights in the role of LPA-mediated signaling in human PDACs, which may facilitate both the interpretation of the upcoming results from the IOA-289 PDAC clinical trial, and identify other high yield targets in the LPA-signaling pathway for future trials.

Methods

Clinical and mRNA expression PDAC data was obtained from two well-resourced databases: The Cancer Genome Atlas Program (TCGA) (n=146) via the cBioPortal (<https://www.cbioportal.org>), and a validation cohort of 132 patients, GSE21501 via the Gene Expression Omnibus (GEO) repository of the United States National Institutes of Health (<https://www.ncbi.nlm.nih.gov/geo>) [42, 43]. The expression data

for TCGA was log-transformed using “data_mrna_seq_v2_rsem”, while GSE21501 data was downloaded already normalized and used without any further processing, as previously described [37, 39, 44]. Briefly, after the gene symbols were annotated with the specified Platform (GPL) accession number, the average value was used if the same gene was assigned to multiple probes. Gene expression data from 167 samples of normal pancreatic tissue from Genotype-Tissue Expression (GTEx) was obtained from the University of California Santa Cruz Xena Portal (<https://xena.ucsc.edu>) [45, 46]. As all data was obtained from deidentified databases in the public domain, ethics approval requirements were waived by the Roswell Park Institutional Review Board.

Functional enrichment analysis of genes examined was performed by gene set enrichment analysis (GSEA) [47] on the Molecular Signatures Database Hallmark collection (<http://www.gsea-msigdb.org>) [48]. Gene sets with a false discovery rate (FDR) <0.25 specified enriched signaling [47]. High and low gene expression groups were dichotomized by median gene expression. Positive normalized enriched scores (NES) indicate enriched signaling in the high expression group and negative NES indicate enriched signaling in the low expression group.

The xCell algorithm (<https://xcell.ucsf.edu>) [49] was used to correlate gene expression to the infiltrating fraction of tumor and stromal cells (epithelial cells, endothelial cells, and fibroblasts), and immune cells (CD8+, T helper cell (Th)1 and Th2 cells, T-regulator cells, M1 and M2 macrophages, and dendritic cells) as described [50-53]. The pancreatic cancer mutational landscape (intratumor heterogeneity, homologous recombination defects, fraction genome altered, silent mutation rate, non-silent mutation rate, single-nucleotide neoantigens, and indel mutations) was examined from data derived by Thorsson *et al.* [54]. Immune cytolytic activity (CYT) in the tumor microenvironment was calculated as the geometric mean of the expression of perforin (*PRF1*) and granzyme A (*GZMA*) mRNA expression, which measures the anti-cancer ability of cytotoxic T cells [55].

Statistical analyses and figure production were performed with R-4.2.1 and BioRender ([https://](https://www.biorender.com)

www.biorender.com). mRNA levels for individual genes were dichotomized into low and high groups based on the median expression level. All results are plotted as box plots, with the lower and upper bounds representing the maximum and minimum values, the upper and lower ends of box representing the 25th and 75th percentile values and the bolded bar within the box representing the median value. Two group comparisons were performed using the Mann-Whitney U test and multiple group comparisons by the Kruskal-Wallis test. The R survival software package was used to analyze survival based on high or low gene expression via Cox-proportional hazards regression, and Kaplan-Meier survival curves were compared by the log rank test. $P < 0.05$ was set for statistical significance.

Results

When comparing expression levels between normal pancreatic tissue to PDAC, *ENPP2*, *LPAR1*, *LPAR4*, *LPAR5*, *LPAR6*, *PLPP1*, and *PLPP2* were significantly elevated in the PDAC group, whereas *LPAR2*, *LPAR3*, and *PLPP3* were downregulated (all $P \leq 0.003$) (**Figure 2**). However, within the PDAC tumors, there was no significant correlation between gene expression level and stage of disease (**Figure 3A**). Apart from *PLPP1*, which showed a significant decrease in expression level with grade progression (Grade 1 to 3) ($P = 0.04$), there were no other correlations between tumor grade and gene expression levels (**Figure 3B**). Also, apart from *LPAR5*, which showed higher levels of Ki67 scoring in tumors with high-*LPAR5* expression in both cohorts (all $P \leq 0.005$), there were no consistent correlations between Ki67 scoring and gene expression when dichotomized on the median into low- and high-expression groups (**Figure 3C**).

We next examined survival parameters based on median dichotomized gene expression. The only gene with any statistically significant survival differences in either cohort was *ENPP2*. In the TCGA data, progression-free survival, disease-free survival, disease-specific survival, and overall survival favored the *ENPP2*-high expressing group, with hazard ratios (HRs) ranging from 0.25-0.47 (all $P < 0.001$, **Figure 4**). However, in GSE21501 where overall survival was the only recorded metric, there were no

Lysophosphatidic acid signaling in pancreatic ductal adenocarcinoma

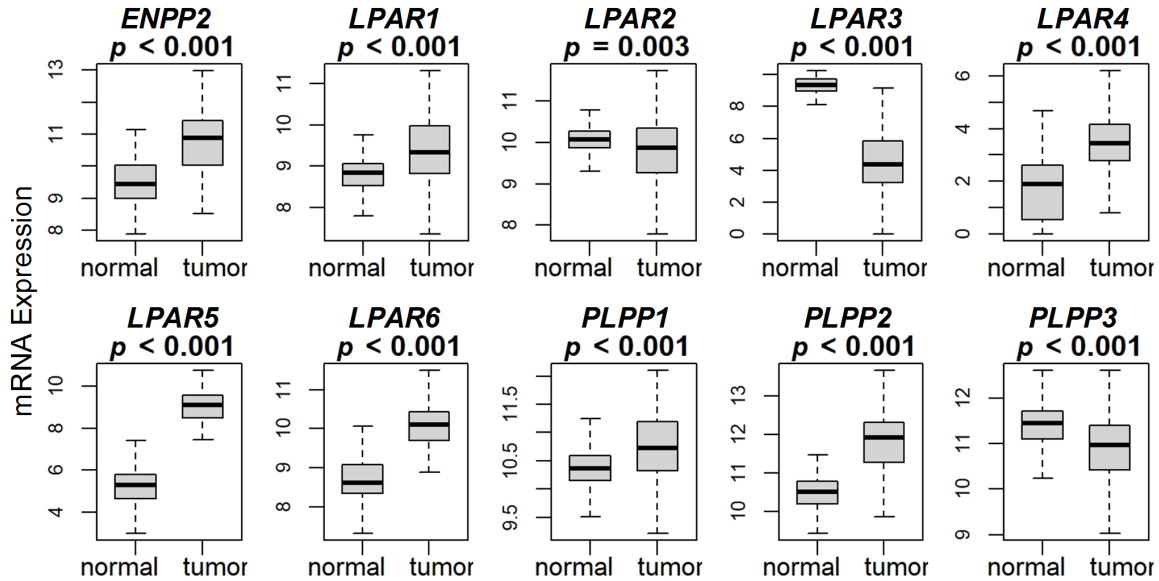


Figure 2. LPA signaling-related gene expression in PDACs compared to normal pancreatic tissues. mRNA expression from 167 normal pancreas in the GTex database is compared to 146 PDACs. Results are plotted as box plots with the bolded center bar within the box plots represents the median, the lower and upper box bounds represent the 25th and 75th percentiles, respectively, and the lower and upper tails represent the minimum and maximum values, respectively.

meaningful differences between the two groups ($P=0.8$, **Figure 4**). We then performed gene set enrichment analyses (GSEA) using the Hallmark gene sets across all genes in both cohorts. Again, *ENPP2* was the only gene with significant normalized enrichment scores (NES) in both cohorts (allograft rejection, complement, and IL6-JAK-STAT3 signaling) (all NES 1.5-2). *LPAR3*, *LPAR4*, *LPAR6*, *PLPP1*, and *PLPP2* had significantly enriched gene sets in at least one cohort, but were not validated in the other cohort (**Figure 5**). There were no enriched gene sets in *LPAR1*, *LPAR2*, *LPAR5*, or *PLPP3* in either cohort. The full GSEA output for all genes by the Hallmark gene set is available in [Supplementary Table 1](#).

Although PDACs tend to have a lower overall tumor mutational burden compared to most cancers, it is a prognostic marker of aggressive tumor biology [56]. We examined common scores of tumor mutational burden by median gene expression. Intratumor heterogeneity scores were not correlated with any of the genes (**Figure 6**). However, high-*ENPP2* expression correlated to lower scores for homologous recombination defects (HRDs), fraction genome altered (FGA), silent mutation rate (SMR), non-silent mutation rate (NSMR), single-nucleotide

variant (SNV) neoantigens, and indel mutations (all $P<0.04$, **Figure 6**). This same pattern occurred also in high-expressing *LPAR1*, *LPAR4*, *PLPP1*, and *PLPP3* tumors (all $P<0.001$), except for indel mutations (**Figure 6**). HRD and FGA were correlated to high-expression *LPAR2* tumors (all $P<0.04$, **Figure 6**). High *LPAR5*-expressing tumors correlated with increased FGA, SMR, NSMR, and indel mutations (all $P<0.04$, **Figure 6**). High *LPAR6*-expressing correlated with lower FGA, SMR, and NSMR scores (all $P\leq 0.04$, **Figure 6**). Finally, high *PLPP2*-expressing tumors correlated to higher scores for HRD, FGA, SMR, NSMR, and SNV neoantigen scores (all $P<0.001$, **Figure 6**).

We next examined gene expression by cybersorted tumor cell populations. Among epithelial cells, representing cancer cells within the PDAC tumor, their levels were decreased in high-expressing *ENPP2*, *LPAR1*, *PLPP1*, and *PLPP3* tumors across both cohorts, while levels were increased in high *LPAR2*, *LPAR5*, and *PLPP2* tumors (all $P<0.02$, **Figure 7A**). The converse was essentially observed for endothelial cells, where their populations were enriched in high-expressing *ENPP2*, *LPAR1*, *LPAR4*, *LPAR6*, *PLPP1*, and *PLPP3* tumors, and in low-expressing *LPAR2* and *PLPP2* tumors in both cohorts

Lysophosphatidic acid signaling in pancreatic ductal adenocarcinoma

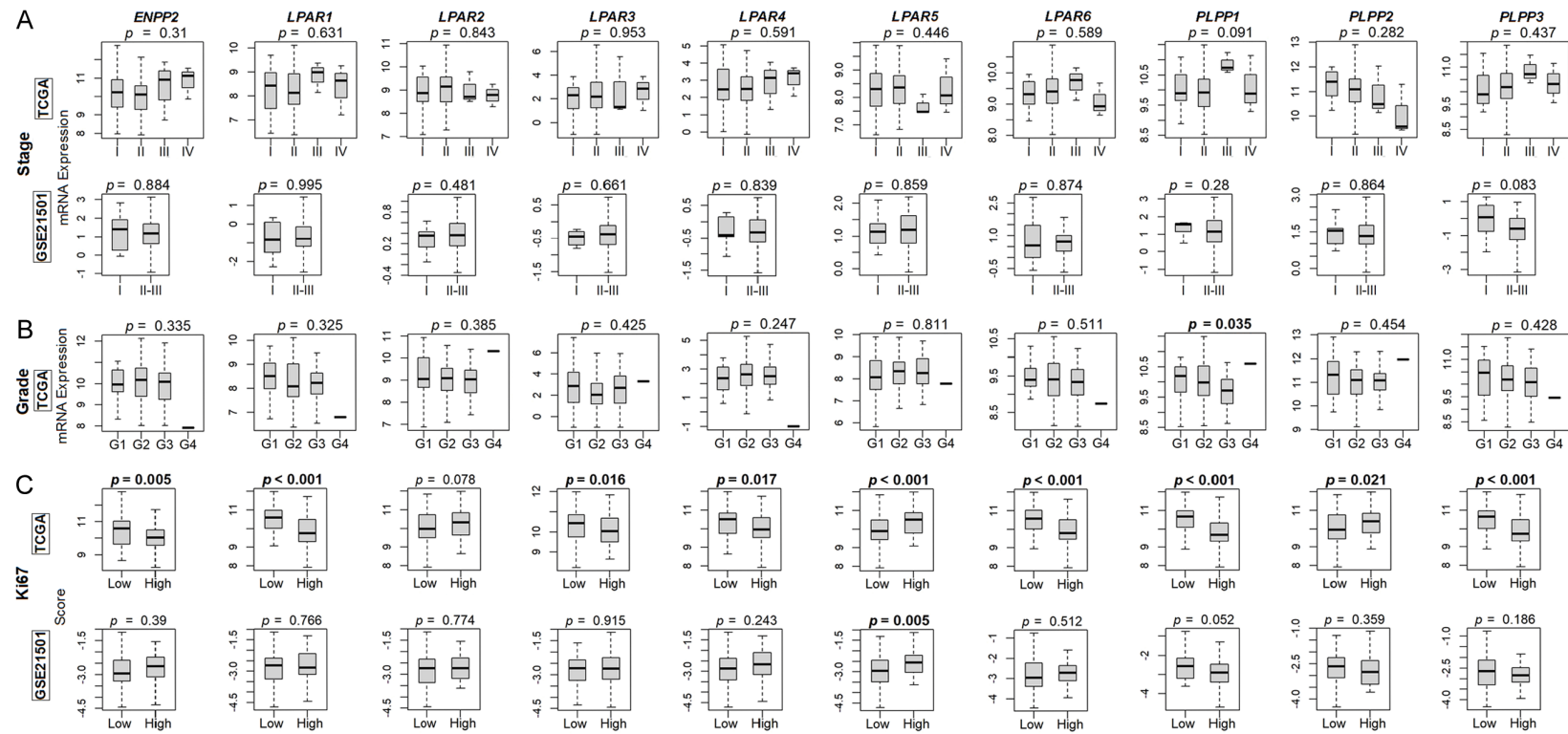


Figure 3. LPA signaling-related gene expression by PDAC characteristics. A. Staging according to the American Joint Committee on Cancer (AJCC). Counts per subgroup. TCGA: I-12, II-127, III-3, IV-3; GSE21501: I-8, II-III-92. B. Grading according AJCC. Grading information not available for GSE21501. Counts per subgroup for TCGA: G1-21, G2-83, G3-41, G4-1. C. Ki67 scoring dichotomized by median gene expression. Results are plotted as box plots with the bolded center bar within the box plots represents the median, the lower and upper box bounds represent the 25th and 75th percentiles, respectively, and the lower and upper tails represent the minimum and maximum values, respectively.

Lysophosphatidic acid signaling in pancreatic ductal adenocarcinoma

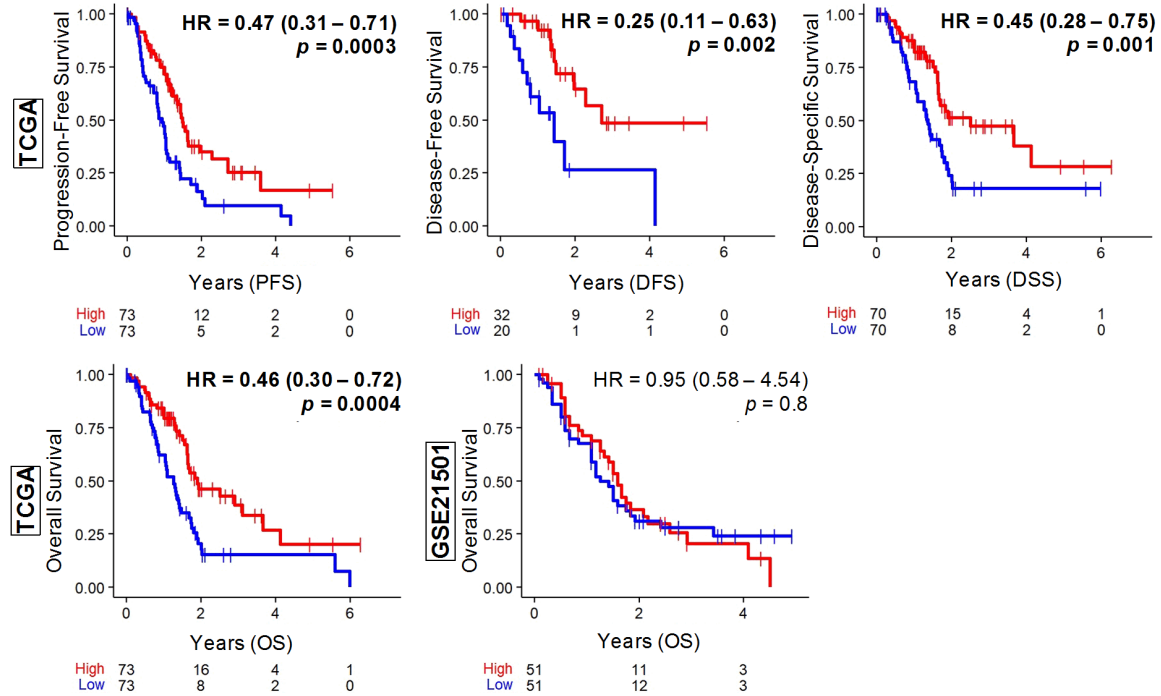


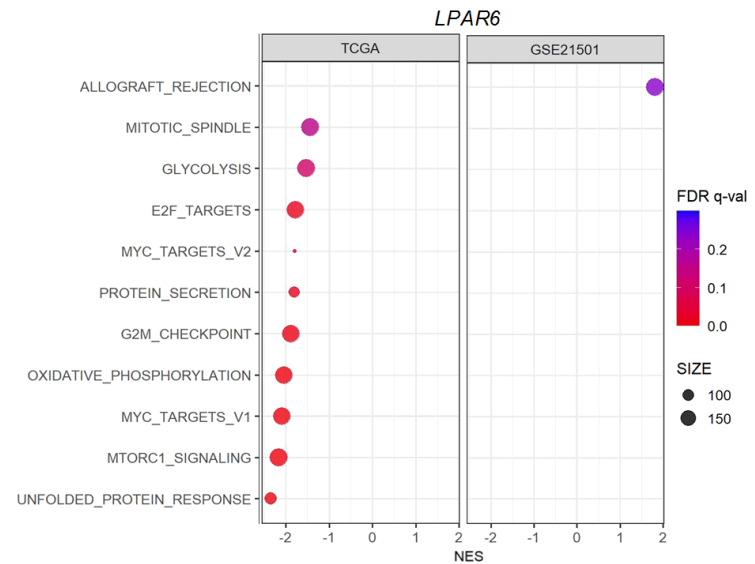
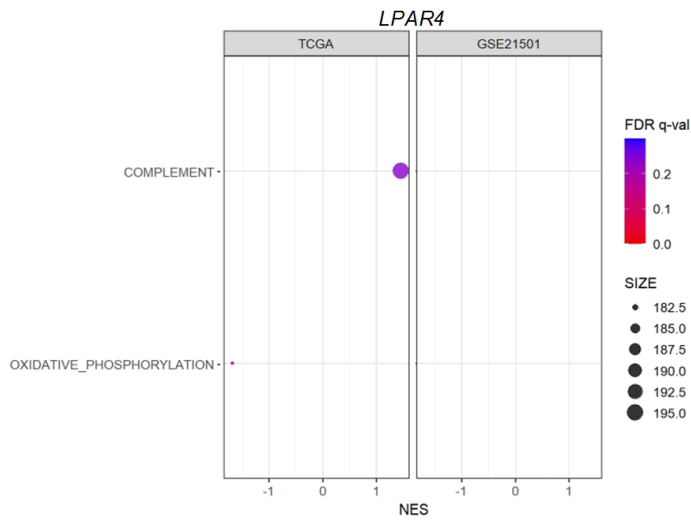
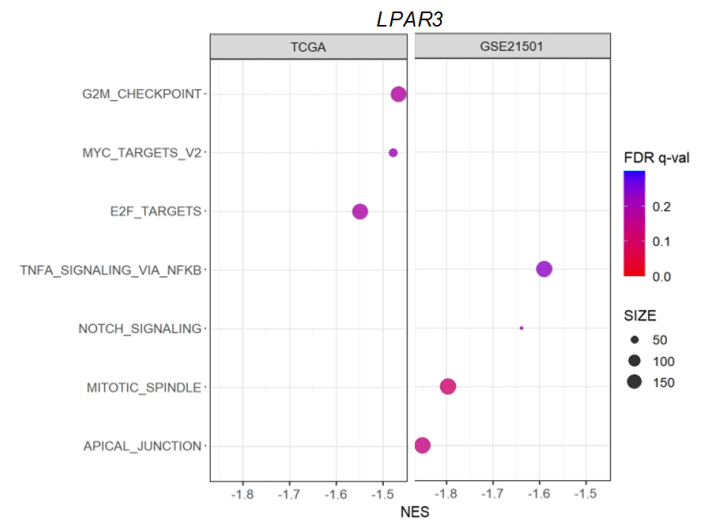
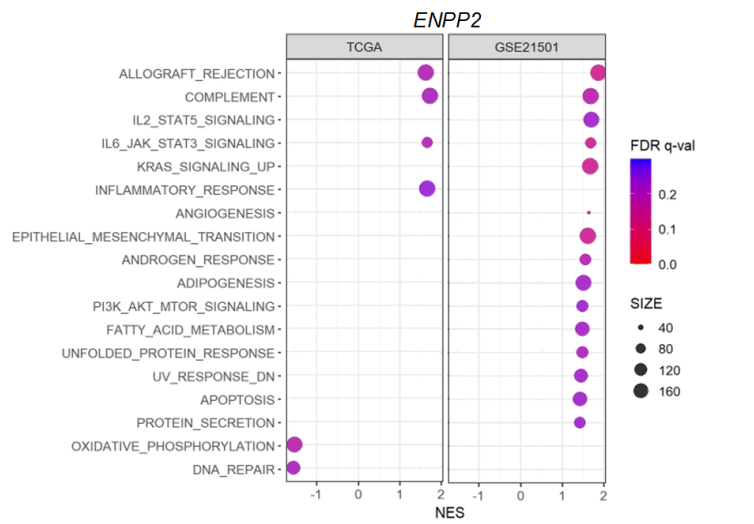
Figure 4. Survival plots for low and high *ENPP2* (ATX) expression in PDACs. First row shows progression-free survival (PFS), disease-free survival (DFS), and disease-specific survival (DSS) for the TCGA cohorts. Second row shows overall survival for the TCGA and GSE21501 cohorts. *ENPP2* expression is dichotomized into low and high groups by the median. The hazard ratio (HR) compares the high group against the low group. *P* values by log rank test. There were no significant findings in survivals for any of the LPAR or LPP genes.

(all $P \leq 0.005$, **Figure 7B**). There was no correlation between gene expression and pericyte levels for any of the genes (not shown). Because PDACs have robust stroma and desmoplastic reactions, we also examined stromal marker scores and fibroblast composition. Stromal fraction was not significantly increased for any genes, but TGF- β response, a surrogate of stromal modulation [57], was significantly elevated in high-expressing *ENPP2*, *LPAR1*, *LPAR4*, and *PLPP3* tumors, and in low-expressing *LPAR2*, *LPAR5*, and *PLPP2* tumors (**Figure 8A**, all $P < 0.05$). TGF- β response mirrored fibroblast composition, with fibroblast enrichment in high-expressing *ENPP2*, *LPAR2*, *LPAR4*, *PLPP1*, and *PLPP3* tumors and in low-expressing *LPAR2*, *LPAR5*, and *PLPP2* tumors across both the TCGA and GSE21501 cohorts (all $P \leq 0.01$, **Figure 8B**).

Lastly, we correlated immune cell populations to gene expression levels. On analysis of prototypical anti-cancerous immune cells, particularly among CD8+ T cells, M1 macrophages, and dendritic cell populations, these cell populations were significantly increased in high-ex-

pressing *ENPP2* and *LPAR1* tumors (all $P < 0.01$, **Figure 9A-D**) across both cohorts. Similar results were also observed in both cohorts of high-expressing *PLPP1* and *PLPP2* tumors for CD8+ T cells and dendritic cells (all $P < 0.01$, **Figure 9A, 9D**). In breast and melanoma models, increased LPAR5-mediated signaling is associated with suppressed tumor CD8+ cell concentrations [28, 58]. In the TCGA cohort, CD8+ T cells were significantly suppressed in *LPAR5*-high tumors, but there was no correlation in the GSE21501 cohort (**Figure 9A**). We also examined pro-cancerous cell populations in the two cohorts, for which no genes were significantly different by medial dichotomization among the regulatory T cell and Th2 cell populations (**Figure 10A, 10B**). However, M2 macrophage levels were significantly elevated in high-expressing *ENPP2* and *PLPP3* tumors in both cohorts (all $P < 0.001$, **Figure 10C**). On examination of immune scores by Thorsson et al. [54], leukocyte fractions and lymphocyte infiltration scores were increased in high-expressing *ENPP2*, *LPAR1*, *LPAR4*, *PLPP1*, and *PLPP3* tumors, and decreased in high-expressing *LPAR2*, *LPAR5*, and *PLPP2* tumors (all

Lysophosphatidic acid signaling in pancreatic ductal adenocarcinoma



Lysophosphatidic acid signaling in pancreatic ductal adenocarcinoma

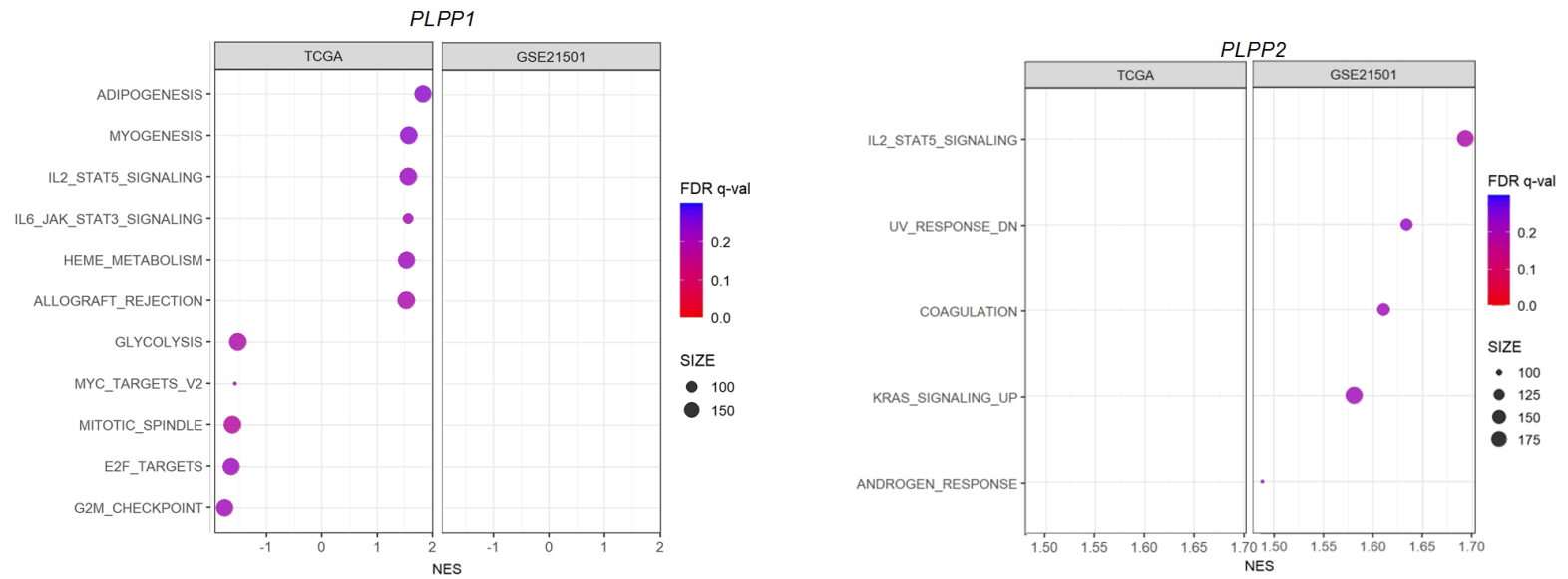
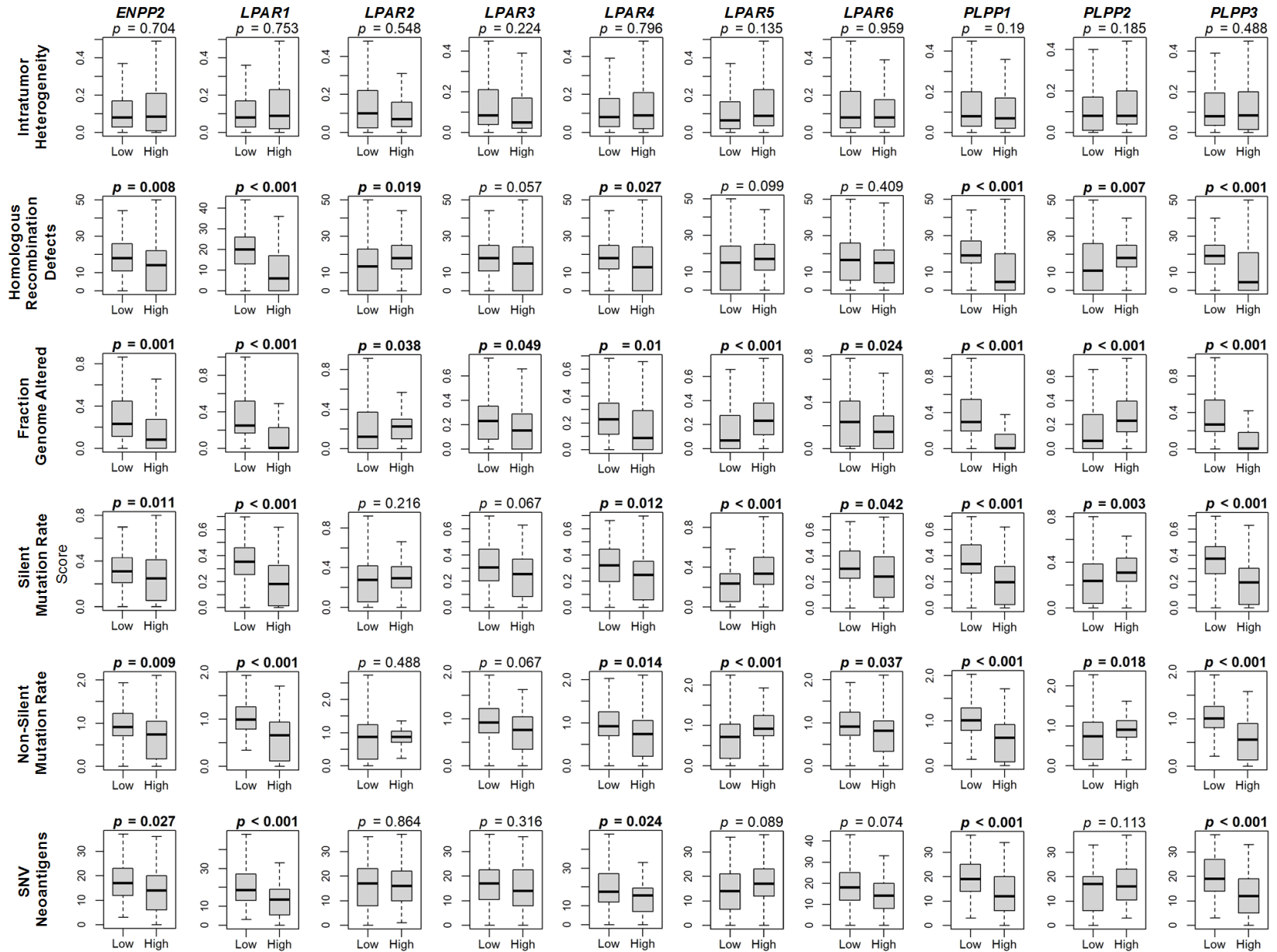


Figure 5. Gene set enrichment analysis (GSEA) for LPA signaling-related expression. GSEA results from the Hallmark gene sets in genes and cohorts that reached significance. A false discovery rate (FDR) of less than 0.25 was considered statistically significant (illustrated by the color of the dot). Dot size represents number of genes in the gene set after filtering out those genes not in the expression dataset. There were no significantly enriched gene sets in either of the cohorts for *LPAR1*, *LPAR2*, *LPAR5*, or *PLPP3*.

Lysophosphatidic acid signaling in pancreatic ductal adenocarcinoma



Lysophosphatidic acid signaling in pancreatic ductal adenocarcinoma

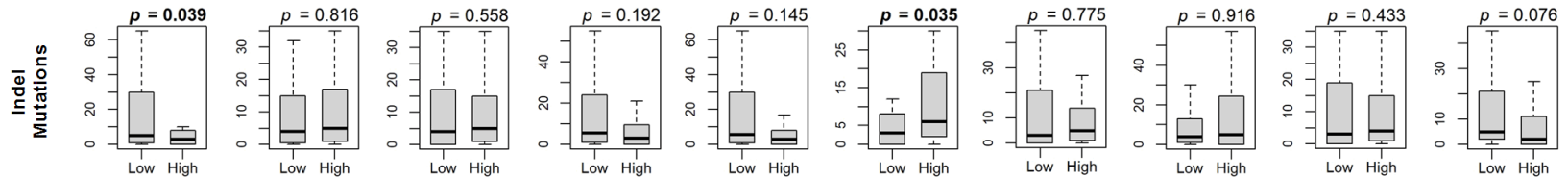
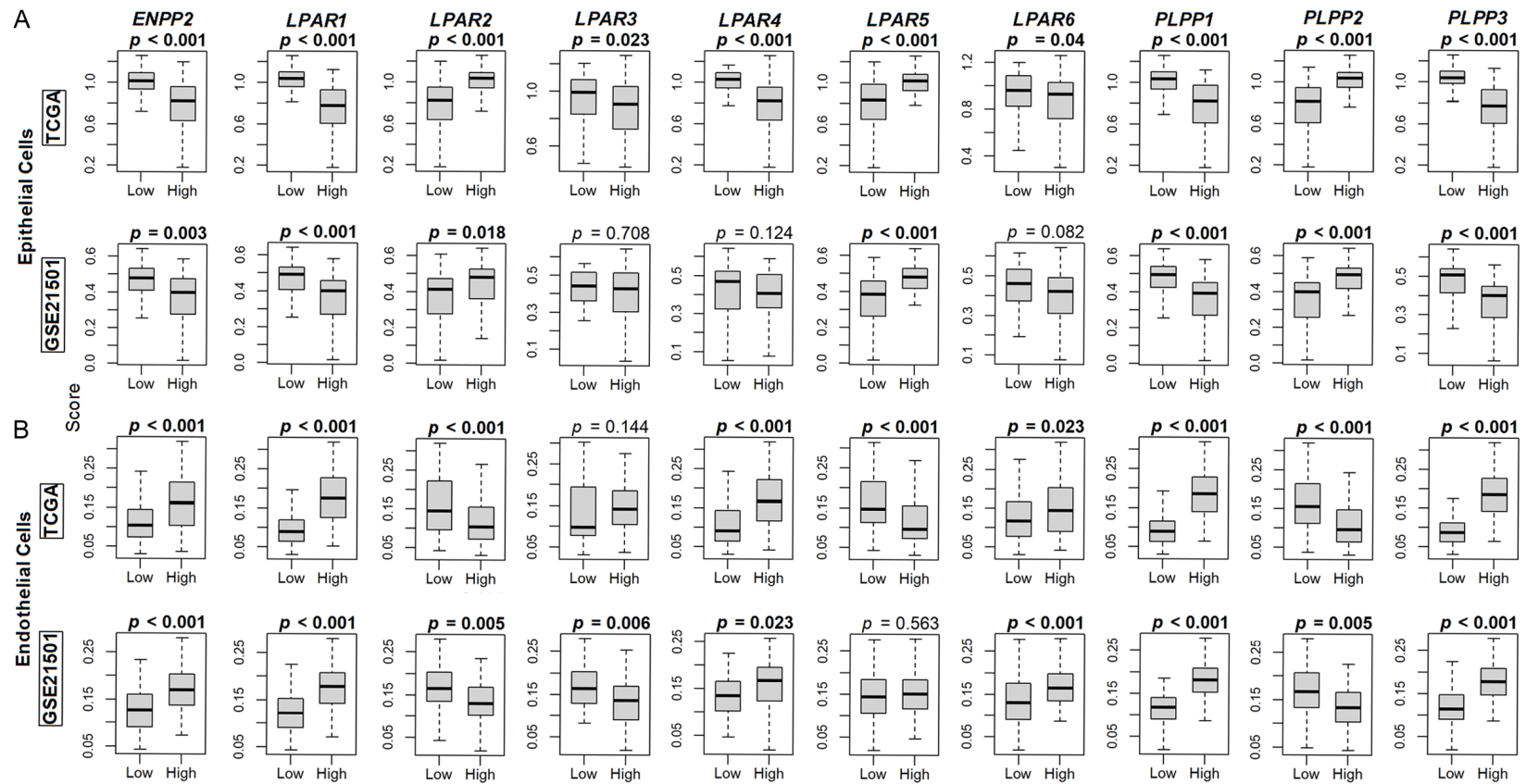


Figure 6. LPA signaling-related gene expression association with PDAC mutations. Box plots of intratumor heterogeneity, homologous recombination defects, fraction genome altered, silent mutation rate, non-silent mutation rate, single-nucleotide variant (SNV) neoantigens, and indel mutations. Data is based on the scores by Thorsson, *et al.* [54]. Gene expression is dichotomized by median expression. Results are plotted as box plots with the bolded center bar within the box plots represents the median, the lower and upper box bounds represent the 25th and 75th percentiles, respectively, and the lower and upper tails represent the minimum and maximum values, respectively.



Lysophosphatidic acid signaling in pancreatic ductal adenocarcinoma

Figure 7. Epithelial and endothelial composition correlation with LPA signaling-related gene expression in PDAC. A. Box plots of epithelial cell composition based on the xCell algorithm for the TCGA and GSE21501 cohorts. B. Box plots of endothelial cell composition based on the xCell algorithm for the TCGA and GSE21501 cohorts. Results are plotted as box plots with the bolded center bar within the box plots represents the median, the lower and upper box bounds represent the 25th and 75th percentiles, respectively, and the lower and upper tails represent the minimum and maximum values, respectively.

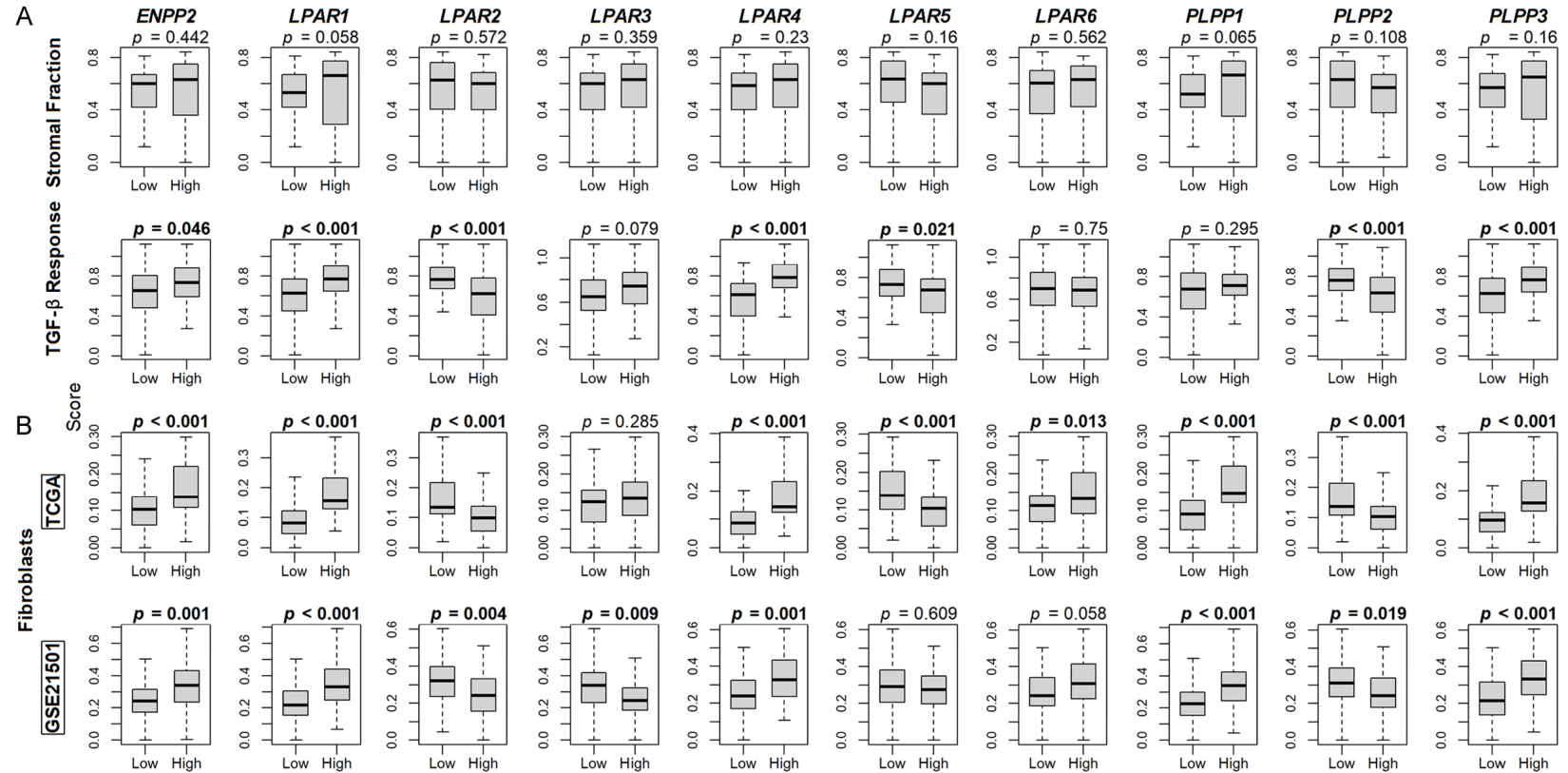
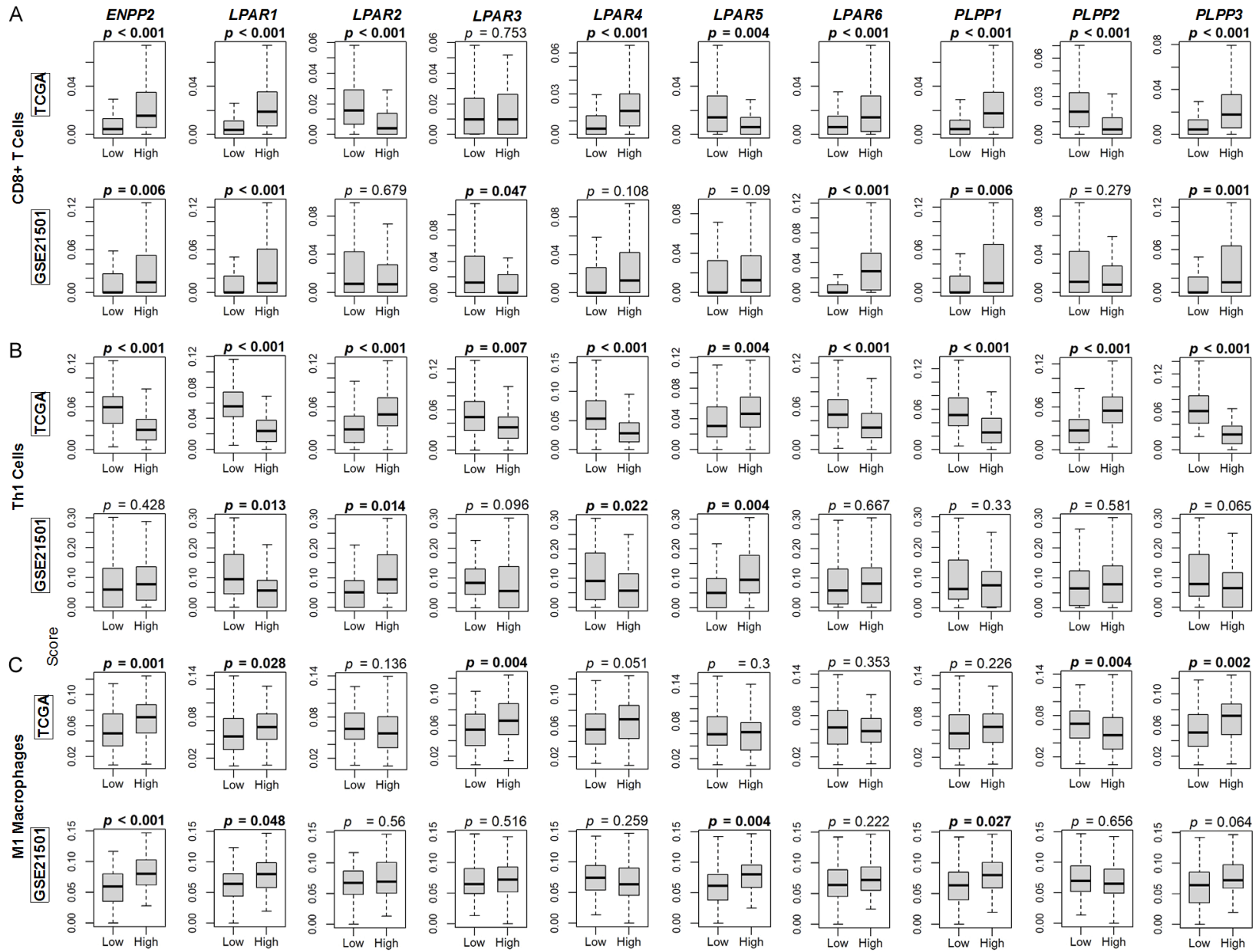


Figure 8. Stromal related scores and fibroblast composition correlation with LPA signaling-related gene expression in PDAC. A. Box plots of calculated scores for stromal fraction and TGF-β response, based on the scores by Thorsson, *et al.* [54]. B. Box plots of fibroblast cell composition based on the xCell algorithm for the TCGA and GSE21501 cohorts. Results are plotted as box plots with the bolded center bar within the box plots represents the median, the lower and upper box bounds represent the 25th and 75th percentiles, respectively, and the lower and upper tails represent the minimum and maximum values, respectively.

Lysophosphatidic acid signaling in pancreatic ductal adenocarcinoma



Lysophosphatidic acid signaling in pancreatic ductal adenocarcinoma

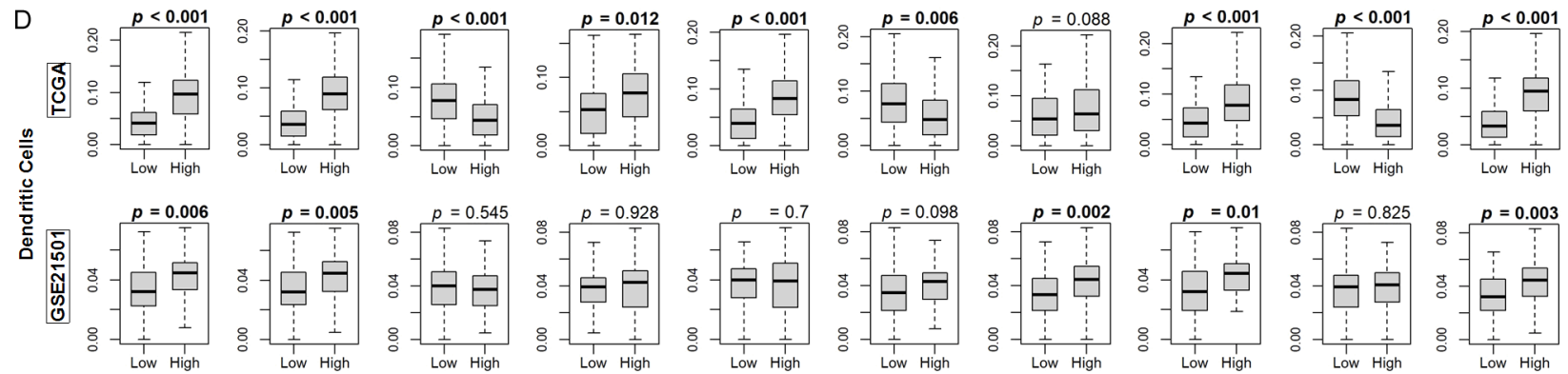


Figure 9. Anti-cancerous immune cell correlation with LPA signaling-related gene expression in PDAC. A. Box plots of CD8+ cell composition based on the xCell algorithm for the TCGA and GSE21501 cohorts. B. Box plots of Th1 cell composition based on the xCell algorithm for the TCGA and GSE21501 cohorts. C. Box plots of M1 macrophage cell composition based on the xCell algorithm for the TCGA and GSE21501 cohorts. D. Box plots of dendritic cell composition based on the xCell algorithm for the TCGA and GSE21501 cohorts. Results are plotted as box plots with the bolded center bar within the box plots represents the median, the lower and upper box bounds represent the 25th and 75th percentiles, respectively, and the lower and upper tails represent the minimum and maximum values, respectively.

Lysophosphatidic acid signaling in pancreatic ductal adenocarcinoma



Lysophosphatidic acid signaling in pancreatic ductal adenocarcinoma

Figure 10. Pro-cancerous immune cell correlation with LPA signaling-related gene expression in PDAC. A. Box plots of regulatory T cell composition based on the xCell algorithm for the TCGA and GSE21501 cohorts. B. Box plots of Th2 cell composition based on the xCell algorithm for the TCGA and GSE21501 cohorts. C. Box plots of M2 macrophage cell composition based on the xCell algorithm for the TCGA and GSE21501 cohorts. Results are plotted as box plots with the bolded center bar within the box plots represents the median, the lower and upper box bounds represent the 25th and 75th percentiles, respectively, and the lower and upper tails represent the minimum and maximum values, respectively.

$P \leq 0.01$, **Figure 11**). Tumor infiltration lymphocyte (TIL) fraction was increased in high expressing *ENPP2* and *LPAR3* tumors (all $P < 0.04$, **Figure 11**). Macrophage regulation scores were significantly different for all genes: increased in high-expressing *ENPP2*, *LPAR1*, *LPAR3*, *LPAR4*, *LPAR6*, *PLPP1*, and *PLPP3* tumors, and decreased in high-expressing *LPAR2*, *LPAR5*, and *PLPP2* tumors. Wound healing scores, which typically relate to decreased overall survival [54], tended to have an opposite relation compared to the other scores, particularly, decreased in high-expressing *ENPP2*, *LPAR1*, *LPAR6*, *PLPP1*, and *PLPP3* tumors (all $P < 0.01$, **Figure 11**). Across both cohorts, cytolytic (CYT) scores were increased in high-expressing *ENPP2*, *LPAR1*, *LPAR6*, *PLPP1*, and *PLPP3* tumors (all $P < 0.01$, **Figure 12**). CYT scores were decreased in high-expressing *LPAR2* and *PLPP2* tumors in the TCGA cohort (all $P < 0.001$), but did not reach significance in the GSE21501 cohort (**Figure 12**).

Discussion

The LPA pathway has been extensively researched for more than 30 years as a potentially druggable target at multiple levels. The goal of targeting LPA signaling has been primarily to mitigate the development of cancer therapy resistance either through blockade of resistance mechanisms or by potentiating therapeutic synergism with conventional therapies. Multiple agents against the LPA axis players have been developed and tested primarily pre-clinically against cancer and other diseases of chronic inflammation. However, the ATX inhibitor IOA-289 has become the first agent to enter clinical trials for cancer. It is currently being investigated in a phase 1b, open label, dose-escalation study in combination with gemcitabine/nab-paclitaxel in patients with metastatic PDAC, with preliminary results showing a reduction in CA19-9 of greater than 50%, and durable partial responses beyond those achieved in the control cohorts [59]. Hence, our

motivation for this study was to survey expression patterns of the LPA-related signaling pathway genes within the PDAC TME in order to predict future directions of research for ongoing LPA-pathway targeting therapeutic interventions.

In the study, we showed that *ENPP2*, *LPAR1*, *LPAR4*, *LPAR5*, *LPAR6*, and *PLPP1* were upregulated in PDAC compared to normal pancreatic tissue. No genes showed a strong correlation to either disease stage or grade. Only *ENPP2* showed consistent upregulation of immune related and inflammatory gene sets in both cohorts. Like human breast cancers, *ENPP2* expression was enriched in tumor stroma cells (fibroblasts and endothelial cells) rather than tumor epithelial cells [39]. *LPAR2*, *LPAR5*, and *PLPP2* were upregulated in tumor epithelial cells, while *LPAR1*, *PLPP1*, and *PLPP3* were downregulated. Immune cell infiltration scores and CYT scores were significantly increased in high-*ENPP2* expressing tumors, which are typically markers of decreased tumorigenicity. Only *ENPP2* expression correlated to patient survival outcomes, where high *ENPP2* expression tended to have better survival characteristics, particularly in the TCGA cohort. This finding was unexpected according to the conventional model of ATX expression and tumorigenicity, as high tumor ATX expression is predicted to correlate with a more aggressive phenotype [6, 9]. However, we have observed a similar phenotype in high-expressing *ENPP2* early breast cancer tumors [13, 39]. In the TCGA cohort, 95 percent of PDAC patients had early-stage disease (stage I or II), whereas the GSE21501 cohort tended to have higher-stage disease (>90% stage II or III). This likely explains why overall survival favored the high-*ENPP2* group in TCGA but lost significance in the GSE21501 cohort. Additionally, Ki67 scores, a marker of cellular proliferation, were significantly lower in the high-*ENPP2* group in the TCGA group, but trended non-significantly towards being higher in the GSE21501 cohort. This finding would support our similar conclusion in early breast

Lysophosphatidic acid signaling in pancreatic ductal adenocarcinoma

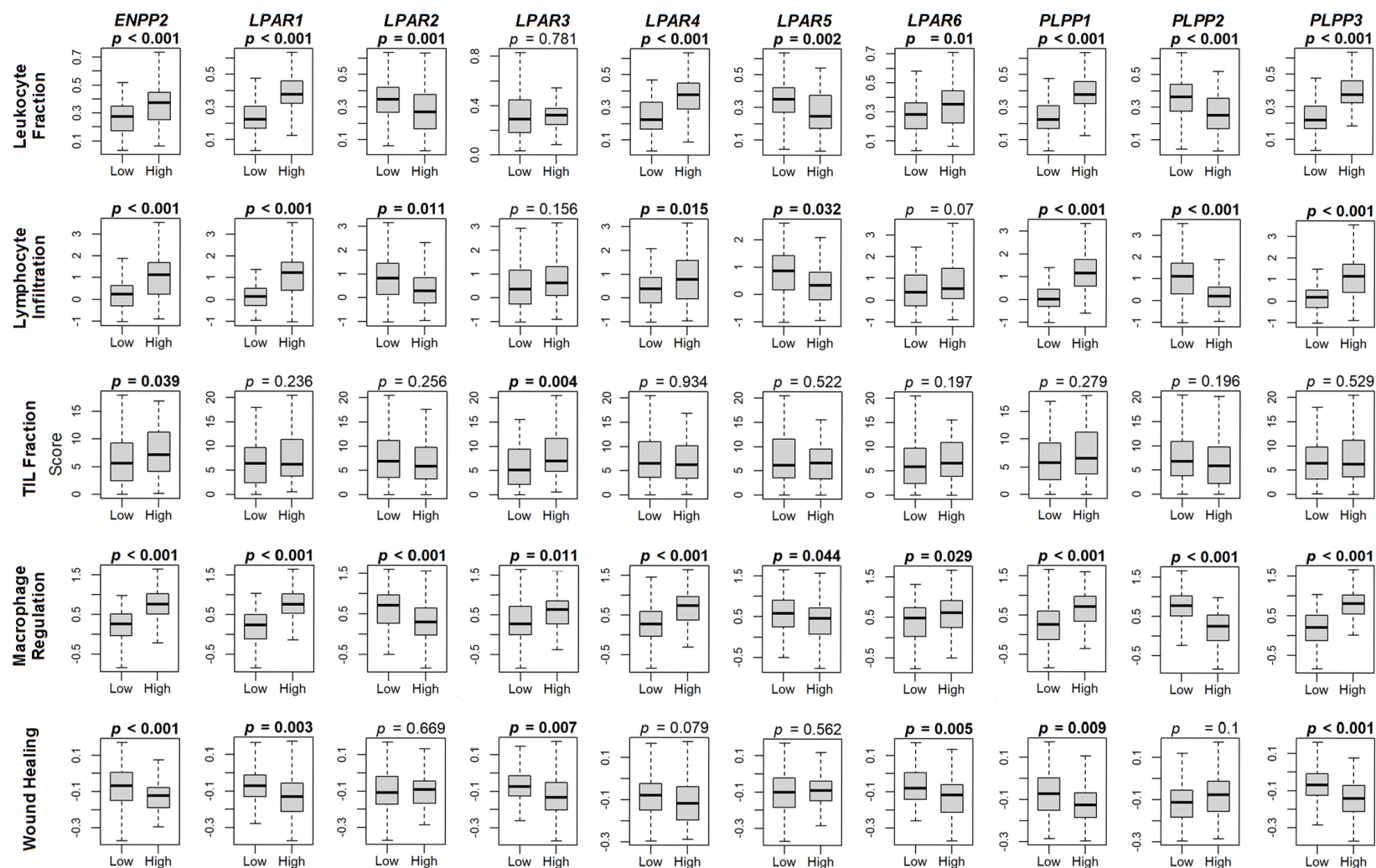


Figure 11. Immune scores for markers of tumor immune cell populations correlation with LPA signaling-related gene expression in PDAC. Box plots of immune scores (leukocyte fraction, lymphocyte infiltration, tumor infiltration leukocyte (TIL) fraction, macrophage regulation, and wound healing) are based on the scores by Thorsson, *et al.* [54]. Results are plotted as box plots with the bolded center bar within the box plots represents the median, the lower and upper box bounds represent the 25th and 75th percentiles, respectively, and the lower and upper tails represent the minimum and maximum values, respectively.

Lysophosphatidic acid signaling in pancreatic ductal adenocarcinoma

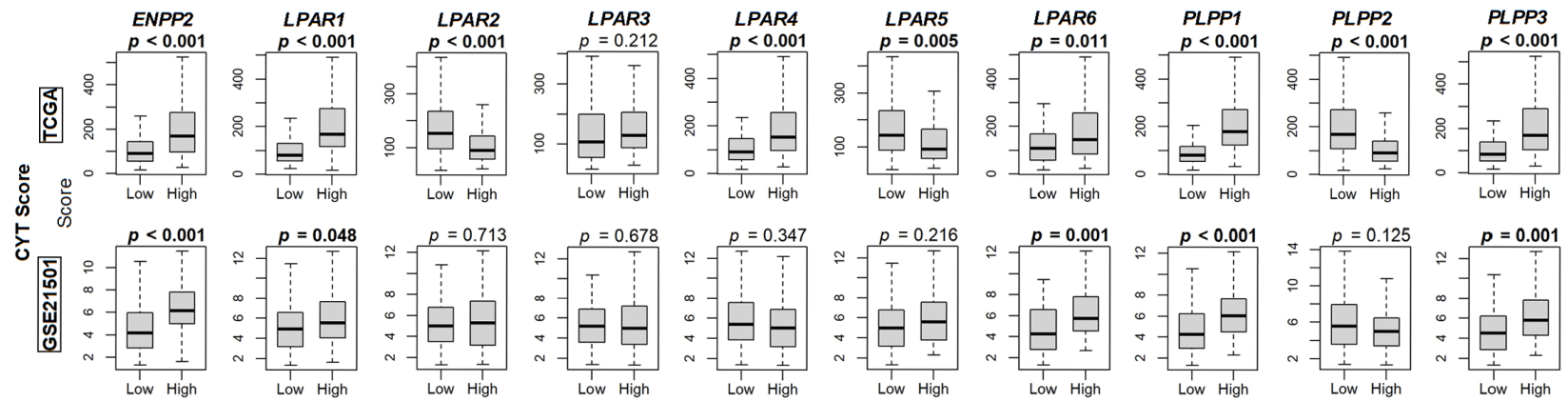


Figure 12. Cytolytic (CYT) score correlation with LPA signaling-related gene expression in PDAC. Box plots of CYT scores based on the xCell algorithm for the TCGA and GSE21501 cohorts. Results are plotted as box plots with the bolded center bar within the box plots represents the median, the lower and upper box bounds represent the 25th and 75th percentiles, respectively, and the lower and upper tails represent the minimum and maximum values, respectively.

cancer where *ENPP2* levels, predominantly expressed in the tumor stroma, may function primarily in a physiological wound healing role to suppress tumor progression [13, 39]. However, at some point, these tumors express their underlying propensity to hijack ATX production and subsequent LPA signaling for progressive tumorigenesis in the context of more advanced or biologically aggressive disease [13, 60].

Recent emerging evidence supports ATX as a promoter of tumor progression in PDAC. Auciello et al. demonstrated that as pancreatic stellate cells transformed into cancer-associated fibroblasts, tumor stroma increased both the LPC concentrations and ATX levels [60]. In both in vitro experiments and murine models, the ATX-LPA axis promoted PDAC cell proliferation, migration, and AKT activation, all of which could be suppressed with potent oral ATX inhibition, resulting in suppressed tumor growth [60]. ATX in the PDAC TME can suppress the infiltration of eosinophils into the TME, thereby shielding the tumor from the immune system, a phenomenon that can be blocked with potent ATX inhibition in murine models [61, 62]. Another group also demonstrated ATX production in inflammatory cancer-associated fibroblasts in PDAC mediates adaptive resistance to TGF- β receptor-mediated inhibition. Treatment with the ATX inhibitor IOA-289 was synergistic with the TGF- β receptor inhibitor galunisertib to improve the efficacy of gemcitabine in PDAC murine models [15]. In breast cancer murine models, IOA-289 treatment both decreased TGF- β 1/ β 2 cytokine signaling and increased anti-tumor CD8 α + T-cell tumor infiltration, resulting in decreased tumor growth [28, 29]. IOA-289 treatment may have similar effects in PDAC.

The majority of ATX in the breast is produced by adipocytes and this is increased by tumor-induced inflammation. Knockout of ATX in adipocytes decreased plasma ATX by ~40%, but this did not affect breast tumor growth [28]. By contrast, treatment with IOA-289 to block total ATX activity decreased tumor growth by ~60%, demonstrating that another source of ATX drives tumor growth [28]. This is likely to come from tumor stromal cells such as fibroblasts, leukocytes or endothelial cells, which express the majority of ATX within mouse [28] and human breast tumors [39]. Similarly, in this study, ATX expression was enriched in tumor

stromal cells compared to pancreatic cancer (epithelial) cells. These observations demonstrate that bulk ATX concentrations are much less important than where the ATX is produced specifically to drive tumor growth and metastasis. This specificity is explained because secreted ATX acts locally by attaching to integrins [11, 63, 64] or syndecan-4 [65] on adjacent cells. Cell-associated ATX acts as a chaperone for LPA by specifically channeling LPA to activate its receptors. The Type IV ATX inhibitors that are in clinical trials are designed to block the binding of LPA to an allosteric tunnel in ATX and diminish this channeling of LPA to its receptors [63]. These inhibitors are particularly effective in decreasing the inflammatory cycle, tumor growth and the accumulation of inflammatory macrophages [9, 66]. The recruitment of CD8+ T-cells is also decreased through activation of LPAR5 [67-69]. Thus, inhibition of ATX with a Type IV inhibitor such as IOA-289, increases the accumulation of CD8+ T-cells in breast tumors, which should increase immune-surveillance [28, 29]. Similar biological effects are predicted to occur in PDACs with IOA-289, though confirmatory investigations are required.

Regarding the LPARs in PDACs, there is a paucity of literature and virtually none concerning the LPPs. In PDAC cell cultures, *LPAR2* and *LPAR3* levels significantly increased in response to hypoxic conditions (5% or less oxygen) [70, 71]. Similarly, cultured PDAC cells increased *LPAR2* expression following exposure to X-ray radiation or oxidative stress following exposure to hydrogen peroxide, with cell motility and survival rates increased following treatment with *LPAR2* agonists [72]. *LPAR1* signaling has been shown to interact with β -catenin signaling pathway mediators to promote invasion in cell culture assays [73]. Short-hairpin RNA knockdown of *LPAR4* and *LPAR5* has been reported to enhance cell motility and invasion of PDAC cultured cells, whereas knockdown of *LPAR6* inhibited these tumorigenic traits [74]. In this study, we showed that *LPAR2* expression was predominantly enriched in the epithelial cell portion of PDAC tumors. We showed a similar result in human breast tumors, and *LPAR2*-overexpressing breast cancer cells have the most tumorigenic properties of any the LPARs in both in vitro and pre-clinical animal models [13, 40, 75]. Therefore, selective *LPAR2*-inhibition, in combination with

potent ATX inhibition [76], is likely to provide the most robust blockage of the LPA signaling axis [13]. Finally, with respect to the LPPs, human PDAC tumors demonstrate the classical low PLPP1/3, high PLPP2 expression profile seen in multiple other types of malignancies. While there are currently no known LPP2 inhibitors, or specific pharmacological inducers of LPP1/LPP3 expression to increase LPA turnover in the TME, developing such compounds would be a novel area of investigation [13].

As a retrospective analysis, our study does have several limitations. Although we use two independent cohorts to validate our key findings, the two cohorts are relatively small, and comprised of heterogeneous patient populations and treatments with varied outcomes. Bioinformatics data cannot be used to necessarily imply mechanisms of action, but their utility is to provide comparative analysis to experimental pre-clinical models and insightful perspectives for designing future investigations. The findings of this study should be interpreted as hypothesis generating, and will require multi-omics analysis to validate and delineate the mechanisms of action of the mediators of LPA signaling in the PDAC TME. Critical to future LPA-targeting pharmacological development for PDAC and other malignancies will be determining conditions where the physiological wound healing effects of LPA signaling are subverted into maladaptive effects that promote tumor progression. This is likely a phenomenon that occurs across multiple tumor sites once disease progresses beyond early stages. Under such conditions, inhibitors of ATX-LPA signaling in combination with other treatments might have the largest therapeutic opportunity.

Acknowledgements

This research was supported by the National Institutes of Health, USA (grant numbers R37CA248018, R01CA250412, R01CA251545, R01EB029596), the US Department of Defense BCRP (grant numbers W81XWH-19-1-0674 and W81XWH-19-1-0111 to K.T.), and the National Cancer Institute Cancer Center Support Grant P30CA016056 to Roswell Park Comprehensive Cancer Center and to DNB from the Canadian Institutes of Health Research (PJT-169140).

Disclosure of conflict of interest

D.N.B. is a member of the Scientific and Clinical Advisory Boards of iOnctura and receives funding for a postdoctoral fellow from iOnctura to work on IOA-289.

Address correspondence to: Dr. Kazuaki Takabe, Department of Surgical Oncology, Roswell Park Comprehensive Cancer Center, Elm and Carlton Streets, Buffalo, New York 14263, USA. Tel: 1-716-845-5540; E-mail: kazuaki.takabe@roswellpark.org

References

- [1] Siegel RL, Miller KD, Wagle NS and Jemal A. Cancer statistics, 2023. *CA Cancer J Clin* 2023; 73: 17-48.
- [2] Cronin KA, Scott S, Firth AU, Sung H, Henley SJ, Sherman RL, Siegel RL, Anderson RN, Kohler BA, Benard VB, Negoita S, Wiggins C, Cance WG and Jemal A. Annual report to the nation on the status of cancer, part 1: national cancer statistics. *Cancer* 2022; 128: 4251-4284.
- [3] Hosein AN, Brekken RA and Maitra A. Pancreatic cancer stroma: an update on therapeutic targeting strategies. *Nat Rev Gastroenterol Hepatol* 2020; 17: 487-505.
- [4] Thomas D and Radhakrishnan P. Tumor-stromal crosstalk in pancreatic cancer and tissue fibrosis. *Mol Cancer* 2019; 18: 14.
- [5] Merza N, Farooqui SK, Dar SH, Varughese T, Awan RU, Qureshi L, Ansari SA, Qureshi H, McIlvaine J, Vohra I, Nawras Y, Kobeissy A and Hassan M. Folfirinox vs. gemcitabine + nab-paclitaxel as the first-line treatment for pancreatic cancer: a systematic review and meta-analysis. *World J Oncol* 2023; 14: 325-339.
- [6] Benesch MG, Ko YM, McMullen TP and Brindley DN. Autotaxin in the crosshairs: taking aim at cancer and other inflammatory conditions. *FEBS Lett* 2014; 588: 2712-2727.
- [7] Hemmings DG and Brindley DN. Signalling by lysophosphatidate and its health implications. *Essays Biochem* 2020; 64: 547-563.
- [8] Ikeda H, Takai M and Tsujiuchi T. Lysophosphatidic acid (LPA) receptor-mediated signaling and cellular responses to anticancer drugs and radiation of cancer cells. *Adv Biol Regul* 2024; 92: 101029.
- [9] Benesch MGK, MacIntyre ITK, McMullen TPW and Brindley DN. Coming of age for autotaxin and lysophosphatidate signaling: clinical applications for preventing, detecting and targeting tumor-promoting inflammation. *Cancers (Basel)* 2018; 10: 73.
- [10] Zhang X, Li M, Yin N and Zhang J. The expression regulation and biological function of autotaxin. *Cells* 2021; 10: 939.

Lysophosphatidic acid signaling in pancreatic ductal adenocarcinoma

- [11] Fulkerson Z, Wu T, Sunkara M, Kooi CV, Morris AJ and Smyth SS. Binding of autotaxin to integrins localizes lysophosphatidic acid production to platelets and mammalian cells. *J Biol Chem* 2011; 286: 34654-34663.
- [12] Meduri B, Pujar GV, Durai Ananda Kumar T, Akshatha HS, Sethu AK, Singh M, Kanagarla A and Mathew B. Lysophosphatidic acid (LPA) receptor modulators: structural features and recent development. *Eur J Med Chem* 2021; 222: 113574.
- [13] Benesch MGK, Tang X, Brindley DN and Takabe K. Autotaxin and lysophosphatidate signaling: prime targets for mitigating therapy resistance in breast cancer. *World J Oncol* 2024; 15: 1-13.
- [14] Tang X, Benesch MG and Brindley DN. Lipid phosphate phosphatases and their roles in mammalian physiology and pathology. *J Lipid Res* 2015; 56: 2048-2060.
- [15] Pietrobono S, Sabbadini F, Bertolini M, Mangiameli D, De Vita V, Fazzini F, Lunardi G, Casalino S, Scarlato E, Merz V, Zecchetto C, Quinzii A, Di Conza G, Lahn M and Melisi D. Autotaxin Secretion is a stromal mechanism of adaptive resistance to TGF β inhibition in pancreatic ductal adenocarcinoma. *Cancer Res* 2024; 84: 118-132.
- [16] Benesch MG, Zhao YY, Curtis JM, McMullen TP and Brindley DN. Regulation of autotaxin expression and secretion by lysophosphatidate and sphingosine 1-phosphate. *J Lipid Res* 2015; 56: 1134-1144.
- [17] Euer N, Schwirzke M, Evtimova V, Burtscher H, Jarsch M, Tarin D and Weidle UH. Identification of genes associated with metastasis of mammary carcinoma in metastatic versus non-metastatic cell lines. *Anticancer Res* 2002; 22: 733-740.
- [18] Castellana B, Escuin D, Peiró G, Garcia-Valdecasas B, Vázquez T, Pons C, Pérez-Olabarria M, Barnadas A and Lerma E. ASPN and GJB2 are implicated in the mechanisms of invasion of ductal breast carcinomas. *J Cancer* 2012; 3: 175-183.
- [19] Magkrioti C, Oikonomou N, Kaffe E, Mouratis MA, Xylourgidis N, Barbayianni I, Megadoukas P, Harokopos V, Valavanis C, Chun J, Kosma A, Stathopoulos GT, Bouros E, Bouros D, Syrigos K and Aidinis V. The Autotaxin-lysophosphatidic acid axis promotes lung carcinogenesis. *Cancer Res* 2018; 78: 3634-3644.
- [20] Tang X, Cromwell CR, Liu R, Godbout R, Hubbard BP, McMullen TPW and Brindley DN. Lipid phosphate phosphatase-2 promotes tumor growth through increased c-Myc expression. *Theranostics* 2022; 12: 5675-5690.
- [21] Tang X, Benesch MG, Dewald J, Zhao YY, Patwardhan N, Santos WL, Curtis JM, McMullen TP and Brindley DN. Lipid phosphate phosphatase-1 expression in cancer cells attenuates tumor growth and metastasis in mice. *J Lipid Res* 2014; 55: 2389-2400.
- [22] Flanagan JM, Funes JM, Henderson S, Wild L, Carey N and Boshoff C. Genomics screen in transformed stem cells reveals RNASEH2A, PPAP2C, and ADARB1 as putative anticancer drug targets. *Mol Cancer Ther* 2009; 8: 249-260.
- [23] Morris KE, Schang LM and Brindley DN. Lipid phosphate phosphatase-2 activity regulates S-phase entry of the cell cycle in Rat2 fibroblasts. *J Biol Chem* 2006; 281: 9297-9306.
- [24] Simonetti J, Ficili M, Sgalla G and Richeldi L. Experimental autotaxin inhibitors for the treatment of idiopathic pulmonary fibrosis. *Expert Opin Investig Drugs* 2024; 33: 133-143.
- [25] Maher TM, Ford P, Brown KK, Costabel U, Cottin V, Danoff SK, Groenvelde I, Helmer E, Jenkins RG, Milner J, Molenberghs G, Penninckx B, Randall MJ, Van Den Blink B, Fieuw A, Vanderrijn C, Rocak S, Seghers I, Shao L, Taneja A, Jentsch G, Watkins TR, Wuyts WA, Kreuter M, Verbruggen N, Prasad N and Wijsenbeek MS; ISABELA 1 and 2 Investigators. Ziritaxestat, a novel autotaxin inhibitor, and lung function in idiopathic pulmonary fibrosis: the ISABELA 1 and 2 randomized clinical trials. *JAMA* 2023; 329: 1567-1578.
- [26] ClinicalTrials.gov. To Evaluate the Efficacy, Safety, and Tolerability of BBT-877 in Patients With IPF. National Institute of Health 2023; <https://clinicaltrials.gov/study/NCT05483907>.
- [27] ClinicalTrials.gov. RESPIRARE - Efficacy and Safety of Cudetaxestat in Patients With Idiopathic Pulmonary Fibrosis (IPF). National Institute of Health 2022; <https://clinicaltrials.gov/study/NCT05373914>.
- [28] Tang X, Morris AJ, Deken MA and Brindley DN. Autotaxin inhibition with IOA-289 decreases breast tumor growth in mice whereas knock-out of autotaxin in adipocytes does not. *Cancers (Basel)* 2023; 15: 2937.
- [29] Deken MA, Niewola-Staszewska K, Peyruchaud O, Mikulčić N, Antolić M, Shah P, Chesty A, Tagliavini A, Nizzardo A, Pergher M, Ziviani L, Milleri S, Pickering C, Lahn M, van der Veen L, Di Conza G and Johnson Z. Characterization and translational development of IOA-289, a novel autotaxin inhibitor for the treatment of solid tumors. *ImmunoOncol Technol* 2023; 18: 100384.
- [30] Benesch MG, Tang X, Maeda T, Ohhata A, Zhao YY, Kok BP, Dewald J, Hitt M, Curtis JM, McMullen TP and Brindley DN. Inhibition of autotaxin delays breast tumor growth and lung metastasis in mice. *FASEB J* 2014; 28: 2655-2666.

Lysophosphatidic acid signaling in pancreatic ductal adenocarcinoma

- [31] Tang X, Wuest M, Benesch MGK, Dufour J, Zhao Y, Curtis JM, Monjardet A, Heckmann B, Murray D, Wuest F and Brindley DN. Inhibition of autotaxin with GLPG1690 increases the efficacy of radiotherapy and chemotherapy in a mouse model of breast cancer. *Mol Cancer Ther* 2020; 19: 63-74.
- [32] Centonze M, Di Conza G, Lahn M, Fabregat I, Dituri F, Gigante I, Serino G, Scialpi R, Carrieri L, Negro R, Pizzuto E and Giannelli G. Autotaxin inhibitor IOA-289 reduces gastrointestinal cancer progression in preclinical models. *J Exp Clin Cancer Res* 2023; 42: 197.
- [33] Von Hoff DD, Ervin T, Arena FP, Chiorean EG, Infante J, Moore M, Seay T, Tjulandin SA, Ma WW, Saleh MN, Harris M, Reni M, Dowden S, Laheru D, Bahary N, Ramanathan RK, Tabernero J, Hidalgo M, Goldstein D, Van Cutsem E, Wei X, Iglesias J and Renschler MF. Increased survival in pancreatic cancer with nab-paclitaxel plus gemcitabine. *N Engl J Med* 2013; 369: 1691-1703.
- [34] ClinicalTrials.gov. A Study to Assess an ATX Inhibitor (IOA-289) in Patients With Metastatic Pancreatic Cancer. National Institute of Health 2022; <https://clinicaltrials.gov/ct2/show/NCT05586516>.
- [35] Hagerty BL, Oshi M, Endo I and Takabe K. High mesothelin expression in pancreatic adenocarcinoma is associated with aggressive tumor features but not prognosis. *Am J Cancer Res* 2023; 13: 4235-4245.
- [36] Chida K, Oshi M, Roy AM, Sato T, Endo I and Takabe K. Pancreatic ductal adenocarcinoma with a high expression of alcohol dehydrogenase 1B is associated with less aggressive features and a favorable prognosis. *Am J Cancer Res* 2023; 13: 3638-3649.
- [37] Benesch MG, Wu R, Menon G and Takabe K. High beta integrin expression is differentially associated with worsened pancreatic ductal adenocarcinoma outcomes. *Am J Cancer Res* 2022; 12: 5403-5424.
- [38] Hagerty BL and Takabe K. Biology of mesothelin and clinical implications: a review of existing literature. *World J Oncol* 2023; 14: 340-349.
- [39] Benesch MG, Wu R, Tang X, Brindley DN, Ishikawa T and Takabe K. Autotaxin production in the human breast cancer tumor microenvironment mitigates tumor progression in early breast cancers. *Am J Cancer Res* 2023; 13: 2790-2813.
- [40] Benesch MGK, Wu R, Tang X, Brindley DN, Ishikawa T and Takabe K. Lysophosphatidic acid receptor signaling in the human breast cancer tumor microenvironment elicits receptor-dependent effects on tumor progression. *Int J Mol Sci* 2023; 24: 9812.
- [41] Benesch MGK, Wu R, Tang X, Brindley DN, Ishikawa T and Takabe K. Decreased lipid phosphate phosphatase 1/3 and increased lipid phosphate phosphatase 2 expression in the human breast cancer tumor microenvironment promotes tumor progression and immune system evasion. *Cancers (Basel)* 2023; 15: 2299.
- [42] Stratford JK, Bentrem DJ, Anderson JM, Fan C, Volmar KA, Marron JS, Routh ED, Caskey LS, Samuel JC, Der CJ, Thorne LB, Calvo BF, Kim HJ, Talamonti MS, Iacobuzio-Donahue CA, Hollingsworth MA, Perou CM and Yeh JJ. A six-gene signature predicts survival of patients with localized pancreatic ductal adenocarcinoma. *PLoS Med* 2010; 7: e1000307.
- [43] Stratford JK, Yan F, Hill RA, Major MB, Graves LM, Der CJ and Yeh JJ. Genetic and pharmacological inhibition of TTK impairs pancreatic cancer cell line growth by inducing lethal chromosomal instability. *PLoS One* 2017; 12: e0174863.
- [44] Nelson ED, Benesch MG, Wu R, Ishikawa T and Takabe K. High EIF4EBP1 expression reflects mTOR pathway activity and cancer cell proliferation and is a biomarker for poor breast cancer prognosis. *Am J Cancer Res* 2024; 14: 227-242.
- [45] GTEx Consortium. The Genotype-Tissue Expression (GTEx) project. *Nat Genet* 2013; 45: 580-585.
- [46] Goldman MJ, Craft B, Hastie M, Repčeka K, McDade F, Kamath A, Banerjee A, Luo Y, Rogers D, Brooks AN, Zhu J and Haussler D. Visualizing and interpreting cancer genomics data via the Xena platform. *Nat Biotechnol* 2020; 38: 675-678.
- [47] Subramanian A, Tamayo P, Mootha VK, Mukherjee S, Ebert BL, Gillette MA, Paulovich A, Pomeroy SL, Golub TR, Lander ES and Mesirov JP. Gene set enrichment analysis: a knowledge-based approach for interpreting genome-wide expression profiles. *Proc Natl Acad Sci U S A* 2005; 102: 15545-15550.
- [48] Liberzon A, Birger C, Thorvaldsdóttir H, Ghandi M, Mesirov JP and Tamayo P. The molecular signatures database (MSigDB) hallmark gene set collection. *Cell Syst* 2015; 1: 417-425.
- [49] Aran D, Hu Z and Butte AJ. xCell: digitally portraying the tissue cellular heterogeneity landscape. *Genome Biol* 2017; 18: 220.
- [50] Tokumaru Y, Oshi M, Murthy V, Tian W, Yan L, Angarita FA, Nagahashi M, Matsuhashi N, Futamura M, Yoshida K, Miyoshi Y and Takabe K. Low intratumoral genetic neutrophil-to-lymphocyte ratio (NLR) is associated with favorable tumor immune microenvironment and with survival in triple negative breast cancer (TNBC). *Am J Cancer Res* 2021; 11: 5743-5755.

Lysophosphatidic acid signaling in pancreatic ductal adenocarcinoma

- [51] Chouliaras K, Oshi M, Asaoka M, Tokumaru Y, Khoury T, Endo I, Ishikawa T and Takabe K. Increased intratumor heterogeneity, angiogenesis and epithelial to mesenchymal transition pathways in metaplastic breast cancer. *Am J Cancer Res* 2021; 11: 4408-4420.
- [52] Le L, Tokumaru Y, Oshi M, Asaoka M, Yan L, Endo I, Ishikawa T, Futamura M, Yoshida K and Takabe K. Th2 cell infiltrations predict neoadjuvant chemotherapy response of estrogen receptor-positive breast cancer. *Gland Surg* 2021; 10: 154-165.
- [53] Oshi M, Asaoka M, Tokumaru Y, Angarita FA, Yan L, Matsuyama R, Zsiros E, Ishikawa T, Endo I and Takabe K. Abundance of regulatory T cell (Treg) as a predictive biomarker for neoadjuvant chemotherapy in triple-negative breast cancer. *Cancers (Basel)* 2020; 12: 3038.
- [54] Thorsson V, Gibbs DL, Brown SD, Wolf D, Bortone DS, Ou Yang TH, Porta-Pardo E, Gao GF, Plaisier CL, Eddy JA, Ziv E, Culhane AC, Paull EO, Sivakumar IKA, Gentles AJ, Malhotra R, Farshidfar F, Colaprico A, Parker JS, Mose LE, Vo NS, Liu J, Liu Y, Rader J, Dhankani V, Reynolds SM, Bowlby R, Califano A, Cherniack AD, Anastassiou D, Bedognetti D, Mokrab Y, Newman AM, Rao A, Chen K, Krasnitz A, Hu H, Malta TM, Noushmehr H, Pedamallu CS, Bullman S, Ojesina AI, Lamb A, Zhou W, Shen H, Choueiri TK, Weinstein JN, Guinney J, Saltz J, Holt RA, Rabkin CS; Cancer Genome Atlas Research Network, Lazar AJ, Serody JS, Demicco EG, Disis ML, Vincent BG and Shmulevich I. The immune landscape of cancer. *Immunity* 2018; 48: 812-830, e814.
- [55] Wakiyama H, Masuda T, Motomura Y, Hu Q, Tobo T, Eguchi H, Sakamoto K, Hirakawa M, Honda H and Mimori K. Cytolytic activity (CYT) score is a prognostic biomarker reflecting host immune status in hepatocellular carcinoma (HCC). *Anticancer Res* 2018; 38: 6631-6638.
- [56] Fusco MJ, West HJ and Walko CM. Tumor mutation burden and cancer treatment. *JAMA Oncol* 2021; 7: 316.
- [57] Stuelten CH and Zhang YE. Transforming growth factor- β : an agent of change in the tumor microenvironment. *Front Cell Dev Biol* 2021; 9: 764727.
- [58] Lee SC, Dacheux MA, Norman DD, Balázs L, Torres RM, Augelli-Szafran CE and Tigyi GJ. Regulation of tumor immunity by lysophosphatidic acid. *Cancers (Basel)* 2020; 12: 1202.
- [59] Melisi D, Quinzii A, Valente M, Giacomo AMD, Amato G, Simonetti E, Zecchetto C, Casallino S, Leta L, Messineo L, Mendo L, Hammett T, Deken M, Conza GD, Kaur P, Lahn MMF and Maio M. Safety and clinical efficacy of IOA-289, a novel autotaxin inhibitor, plus gemcitabine and nab-paclitaxel (GnP) in patients with previously untreated metastatic pancreatic ductal adenocarcinoma (mPDAC). *J Clin Oncol* 2024; 42: e15130.
- [60] Auciello FR, Bulusu V, Oon C, Tait-Mulder J, Berry M, Bhattacharyya S, Tumanov S, Allen-Petersen BL, Link J, Kendsersky ND, Vringer E, Schug M, Novo D, Hwang RF, Evans RM, Nixon C, Dorrell C, Morton JP, Norman JC, Sears RC, Kamphorst JJ and Sherman MH. A stromal lysolipid-autotaxin signaling axis promotes pancreatic tumor progression. *Cancer Discov* 2019; 9: 617-627.
- [61] Matas-Rico E and Moolenaar WH. Tumor immune escape by autotaxin: keeping eosinophils at bay. *Trends Cancer* 2024; 10: 283-285.
- [62] Bhattacharyya S, Oon C, Diaz L, Sandborg H, Stempinski ES, Saoi M, Morgan TK, López CS, Cross JR and Sherman MH. Autotaxin-lysolipid signaling suppresses a CCL11-eosinophil axis to promote pancreatic cancer progression. *Nat Cancer* 2024; 5: 283-298.
- [63] Salgado-Polo F and Perrakis A. The structural binding mode of the four autotaxin inhibitor types that differentially affect catalytic and non-catalytic functions. *Cancers (Basel)* 2019; 11: 1577.
- [64] Perrakis A and Moolenaar WH. Autotaxin: structure-function and signaling. *J Lipid Res* 2014; 55: 1010-1018.
- [65] Leblanc R, Sahay D, Houssin A, Machuca-Gayet I and Peyruchaud O. Autotaxin-beta interaction with the cell surface via syndecan-4 impacts on cancer cell proliferation and metastasis. *Oncotarget* 2018; 9: 33170-33185.
- [66] Benesch MGK, Yang Z, Tang X, Meng G and Brindley DN. Lysophosphatidate signaling: the tumor microenvironment's new nemesis. *Trends Cancer* 2017; 3: 748-752.
- [67] Matas-Rico E, Frijlink E, van der Haar Avila I, Menegakis A, van Zon M, Morris AJ, Koster J, Salgado-Polo F, de Kivit S, Lanca T, Mazzocca A, Johnson Z, Haanen J, Schumacher TN, Perrakis A, Verbrugge I, van den Berg JH, Borst J and Moolenaar WH. Autotaxin impedes anti-tumor immunity by suppressing chemotaxis and tumor infiltration of CD8(+) T cells. *Cell Rep* 2021; 37: 110013.
- [68] Mathew D, Kremer KN, Strauch P, Tigyi G, Pelanda R and Torres RM. LPA5 is an inhibitory receptor that suppresses CD8 T-cell cytotoxic function via disruption of early TCR signaling. *Front Immunol* 2019; 10: 1159.
- [69] Lee SC, Dacheux MA, Norman DD, Balázs L, Torres RM, Augelli-Szafran CE and Tigyi GJ. Regulation of tumor immunity by lysophosphatidic acid. *Cancers (Basel)* 2020; 12: 1202.
- [70] Takai M, Yashiro N, Hara K, Amano Y, Yamamoto M and Tsujiuchi T. Roles of lysophospha-

Lysophosphatidic acid signaling in pancreatic ductal adenocarcinoma

- tidic acid (LPA) receptor-mediated signaling in cellular functions modulated by endothelial cells in pancreatic cancer cells under hypoxic conditions. *Pathol Res Pract* 2024; 255: 155192.
- [71] Takai M, Okuda A, Amano Y, Yashiro N, Hara K, Yamamoto M and Tsujiuchi T. Effects of LPA receptor-mediated signaling on the modulation of cellular functions of pancreatic cancer cells cultured in fibroblast supernatants under hypoxic conditions. *J Bioenerg Biomembr* 2023; 55: 169-177.
- [72] Okuda A, Takai M, Kurisu R, Takamoto M, Ikeda H and Tsujiuchi T. Roles of lysophosphatidic acid (LPA) receptor-2 (LPA(2)) in the regulation of cellular responses induced by X-ray irradiation and hydrogen peroxide in pancreatic cancer cells. *Int J Radiat Biol* 2023; 99: 1925-1933.
- [73] Shi W, Zhang C, Ning Z, Hua Y, Li Y, Chen L, Liu L, Chen Z and Meng Z. CMTM8 as an LPA1-associated partner mediates lysophosphatidic acid-induced pancreatic cancer metastasis. *Ann Transl Med* 2021; 9: 42.
- [74] Ishii S, Hirane M, Fukushima K, Tomimatsu A, Fukushima N and Tsujiuchi T. Diverse effects of LPA4, LPA5 and LPA6 on the activation of tumor progression in pancreatic cancer cells. *Biochem Biophys Res Commun* 2015; 461: 59-64.
- [75] Liu S, Umezue-Goto M, Murph M, Lu Y, Liu W, Zhang F, Yu S, Stephens LC, Cui X, Murrow G, Coombes K, Muller W, Hung MC, Perou CM, Lee AV, Fang X and Mills GB. Expression of autotaxin and lysophosphatidic acid receptors increases mammary tumorigenesis, invasion, and metastases. *Cancer Cell* 2009; 15: 539-550.
- [76] Banerjee S, Lee S, Norman DD and Tigyi GJ. Designing dual inhibitors of autotaxin-LPAR GPCR axis. *Molecules* 2022; 27: 5487.